Thermochimica Acta 497 (2010) 129–136

Contents lists available at ScienceDirect

Thermochimica Acta

journal homepage: www.elsevier.com/locate/tca

Co-crystal of (*R*,*R*)-*1*,*2*-cyclohexanediol with (*R*,*R*)-tartaric acid, a key structure in resolution of the (±)-*trans*-diol by supercritical extraction, and the related ternary phase system

Paul Thorey[a], Petra Bombicz[b], Imre Miklós Szilágyi[c,d], Péter Molnár[a], György Bánsághi[a], Edit Székely[a], Béla Simándi[a], László Párkányi[b], György Pokol[d], János Madarász[d,*]

[a] *Department of Chemical and Environmental Process Engineering, Budapest University of Technology and Economics, H-1521 Budapest, Hungary*
[b] *Institute of Structural Chemistry, Chemical Research Center, Hungarian Academy of Science, H-1525 Budapest, Hungary*
[c] *Material Structure and Modeling Research Group, Hungarian Academy of Sciences, H-1111 Budapest, Hungary*
[d] *Department of Inorganic and Analytical Chemistry, Budapest University of Technology and Economics, H-1521 Budapest, Hungary*

ARTICLE INFO

Article history:
Received 19 June 2009
Received in revised form 2 September 2009
Accepted 7 September 2009
Available online 13 September 2009

Keywords:
Chiral resolution
(±)-*Trans*-1,2-cyclohexanediol
(*R*,*R*)-Tartaric acid
Single crystal and powder X-ray diffraction (XRD)
Crystal structure determination
FTIR spectroscopy
Differential scanning calorimetry (DSC)
Simultaneous TG/DTA
Binary melting phase diagrams
Eutectic compositions and temperatures
Structure–property relationship

ABSTRACT

A novel co-crystal of *trans*-(*R*,*R*)-1,2-cyclohexanediol and (*R*,*R*)-tartaric acid (with 1:1 molar ratio, **1**) has been found to be a key crystalline compound in the improved resolution of (±)-*trans*-1,2-cyclohexanediol by supercritical fluid extraction. The molecular and crystal structure of this co-crystal, which crystallizes in orthorhombic crystal system (space group $P2_12_12_1$, $a = 6.7033(13)$ Å, $b = 7.2643(16)$, $c = 24.863(5)$, $Z = 4$), has been solved by single crystal X-ray diffraction ($R = 0.064$). The packing arrangement consists of two dimensional layers of sandwich-like sheets, where the inner part is constructed by double layers of tartaric acids which hydrophilicity is "covered" on both upper and bottom side by cyclohexanediols with the hydrophobic cyclohexane rings pointing outward. Thus, a rather complex hydrogen bonding pattern is constructed. The relatively high melting point (133 °C) observed by both simultaneous TG/DTA and DSC, and the main features of FTIR-spectrum of **1** are explained by the increased stability of this crystal structure. DSC studies on binary mixtures of co-crystal **1** with (*R*,*R*)-1,2-cyclohexanediol or (*R*,*R*)-tartaric acid, revealed eutectic temperatures of $T_{eu} = 100$ or 131 °C, respectively. Between (*S*,*S*)-1,2-cyclohexanediol and (*R*,*R*)-tartaric acid a eutectic temperature of $T_{eu} = 85$ °C have also been observed. The phase relations have been confirmed by powder X-ray diffraction, as well.

1. Introduction

Enantiopure products take a growing importance in the field of fine chemistry and pharmaceutical industry. Most enantiomers (in 1992 about 65% [1]) are prepared by classical resolution: stereoselective crystallization with an optically active resolving agent. Generally a salt is formed by an exchange of proton between a base and an acid. For instance (+)-tartaric acid (TA) has been widely used as an acidic resolving agent [1,2]. The use of tartaric acid is not restricted to the resolution of bases. Indeed, in some cases where the existence of a salt was expected, IR spectroscopy did not show an exchange of proton, and the formed compound was a complex or co-crystal rather than a salt [3]. Not ionic interaction, but a strong system of hydrogen bonds was responsible for the co-crystallization, as (+)-tartaric acid (TA) is a good hydrogen bond acceptor and donor. This opened the way for the resolution of compounds without basic properties with (+)-tartaric acid derivatives. Chiral alcohols were screened for the resolution with TA derivatives. Whereas O,O′-dibenzoyl-(2*R*,3*R*)-tartaric acid afforded good enantiomeric excesses [4–6], the resolution with O,O′-di-*p*-toluoyl-(2*R*,3*R*)-tartaric acid was less successful [7] and impossible with TA [8].

(±)-*Trans*-1,2-cyclohexanediol (CHD), an important building block for the pharmaceutical industry [9–11], is a good candidate for resolution with TA followed by supercritical fluid extraction. The method was presented in our previous work [12] and based on three steps [13,14] (see Fig. 1):

- The sample preparation: the stereoselective co-crystallization of (*R*,*R*)-*trans*-1,2-cyclohexanediol with (*R*,*R*)-tartaric acid (TA) forming the co-crystal TA-(*R*,*R*)-CHD 1:1 (**1**), while (*S*,*S*)-*trans*-1,2-cyclohexanediol ((*S*,*S*)-CHD) remains free or "uncocrystallized".

---

[*] Corresponding author. Fax: +36 1 463 3408.
E-mail address: madarasz@mail.bme.hu (J. Madarász).

0040-6031/$ – see front matter © 2009 Elsevier B.V. All rights reserved.
doi:10.1016/j.tca.2009.09.001

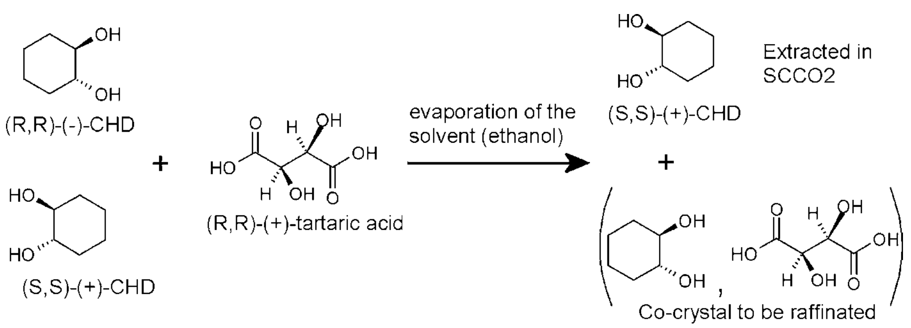

Fig. 1. Scheme of the resolution of (±)-CHD by co-crystal formation followed by an extraction in CO_2 [12].

Table 1
Summary of crystallographic data, data collections, structure determination and refinement for CHD-TA co-crystal (**1**).

Formula	C6 H12 O2, C4 H6 O6
Formula weight	266.24
Crystal system	Orthorhombic
Space group	$P2_12_12_1$ (No. 19)
a, *b*, *c* [Å]	6.7033(13) 7.2643(16) 24.863(5)
V [Å^3]	1210.7(4)
Z, *Z*′	4, 1
D (calc.) [g/cm^3]	1.461
μ (Mo-Kα) [mm^{-1}]	0.128
F(000)	568
Crystal size [mm]	0.55 × 0.55 × 0.34
Temperature [K]	295
Radiation [Å]	Mo-Kα 0.71073
Theta min–max	3.2, 26.4
Dataset	−8:8, −9:9, −31:31
Tot., uniq. data, *R*(int)	25,226, 2468, 0.121
Observed data [$I > 2.0\sigma(I)$]	2216
N_{ref}, N_{par}	2468, 170
R, wR_2, *S* [*]	0.0640, 0.1369, 1.05
Max. and Av. shift/error	0.00, 0.00
Flack *x*	0(1)
Min. and max. resd. dens. [e/Å^3]	−0.26, 0.28

*$w = 1/[\sigma^2(F_o^2) + (0.0222P)^2 + 1.1376P]$ where $P = (F_o^2 + 2F_c^2)/3$.

- The separation, from co-crystal (**1**), of (*S*,*S*)-CHD which is extracted.
- The recovery of (*R*,*R*)-CHD by decomposition of **1**, in this case, by a basic treatment.

The optimization of extraction pressure and temperature led to an improved enantiomeric excess of 62% (yield 50.6%) and 81.9% (yield 33.7%)% for (*S*,*S*)-CHD and (*R*,*R*)-CHD, respectively [12].

In the work of Kawashima and Hirayama the CHD was resolved [15] by reacting with an other resolving agent (*R*,*R*)-1,2-cyclohexanediamine that formed a co-crystal with (*S*,*S*)-CHD preferentially. This method gave (*S*,*S*)-CHD of an optical purity of 67% and the extraction yield was 36.5% based on the racemic compound (for an optical purity of 100% the maximum extraction yield is 50%). The structure of the co-crystal between (*S*,*S*)-CHD and (*R*,*R*)-1,2-cyclohexanediamine was established and discussed in [16–18]. Other co-crystals were found between (*R*,*R*)-CHD and (*R*,*R*)-2,3-diaminobutane [17] or *N*-methylmorphine-*N*-oxide [19]. These structures reveal an inner core based on hydrogen bonds between the diamine and diol moieties, which are responsible for the stereoselectivity of the crystallisation and the geometry of the crystal, and an outer region formed of the hydrophobic groups.

Crystal and molecular structure of the co-crystal (**1**) between (*R*,*R*)-CHD and TA, on which the successful supercritical resolution is based, has been solved by single crystal X-ray diffraction and presented here. This key compound has also been characterized by differential scanning calorimetry (DSC), as well as simultaneous thermogravimetry and differential thermal analysis (TG/DTA), To explore the (in)compatibility of racemic diol with enantiomeric tartaric acid, the various binary phase relations in the ternary (*R*,*R*)-TA-(*R*,*R*)-CHD-(*S*,*S*)-CHD system has been studied by DSC and powder X-ray diffraction (XRD). Based on related eutectic calculations, a schematic ternary phase diagram has also been constructed.

2. Experimental

2.1. Starting materials and sample preparations

(+)-Tartaric acid (>99.5%, Aldrich Ref. No. 251380) was purchased from Sigma–Aldrich. (*S*,*S*)-CHD (>99% for sum of enantiomers, Ref. No. 29003) and (*R*,*R*)-CHD (>99%, Ref. No. 421790) were obtained from Fluka and Aldrich, respectively. Ethanol (>99.5%) was purchased from Reanal Ltd. (Budapest, Hungary).

The transparent single crystals of the co-crystal (**1**) of TA and (*R*,*R*)-CHD were grown by a slow evaporation of the solvent from

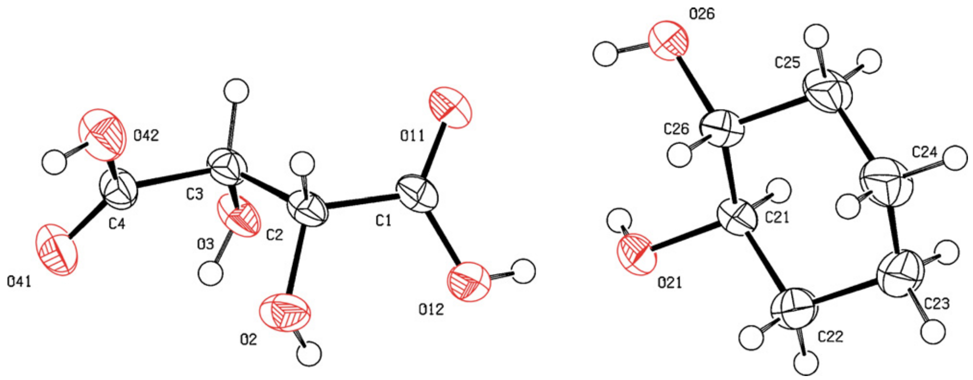

Fig. 2. ORTEP diagram [25] of the CHD-TA co-crystal (**1**), represented at 50% probability level, heteroatoms are shaded. The chiral centers are C2 *R*, C3 *R*, C21 *R* and C26 *R*, respectively.

Table 2
Intermolecular interactions in the crystal structure of CHD-TA co-crystal (**1**).

D–H. . .A	D–H [Å]	H. . .A [Å]	D. . .A [Å]	D–H. . .A [°]	Symmetry operation
O2–H2O. . .O12	0.820	2.300	2.615(3)	104	Intra
O3–H3O. . .O41	0.820	2.380	2.707(3)	105	Intra
O12–H12O. . .O21	0.820	1.770	2.593(3)	176	Within asym. unit
O26–H26O. . .O11	0.820	2.130	2.923(3)	162	Within asym. unit
O2–H2O. . .O26	0.820	2.100	2.873(3)	157	$x, -1+y, z$
O3–H3O. . .O41	0.820	2.020	2.740(4)	146	$(1/2)+x, -(1/2)-y, -z$
O21–H21O. . .O3	0.820	1.970	2.786(3)	171	$(1/2)+x, (1/2)-y, -z$
O26–H26O. . .O41	0.820	2.500	2.882(3)	109	$(1/2)+x, (1/2)-y, -z$
O42–H42O. . .O26	0.820	1.990	2.773(3)	160	$-1+x, -1+y, z$
C2–H2. . .O21	0.980	2.390	3.280(4)	150	$-1+x, y, z$

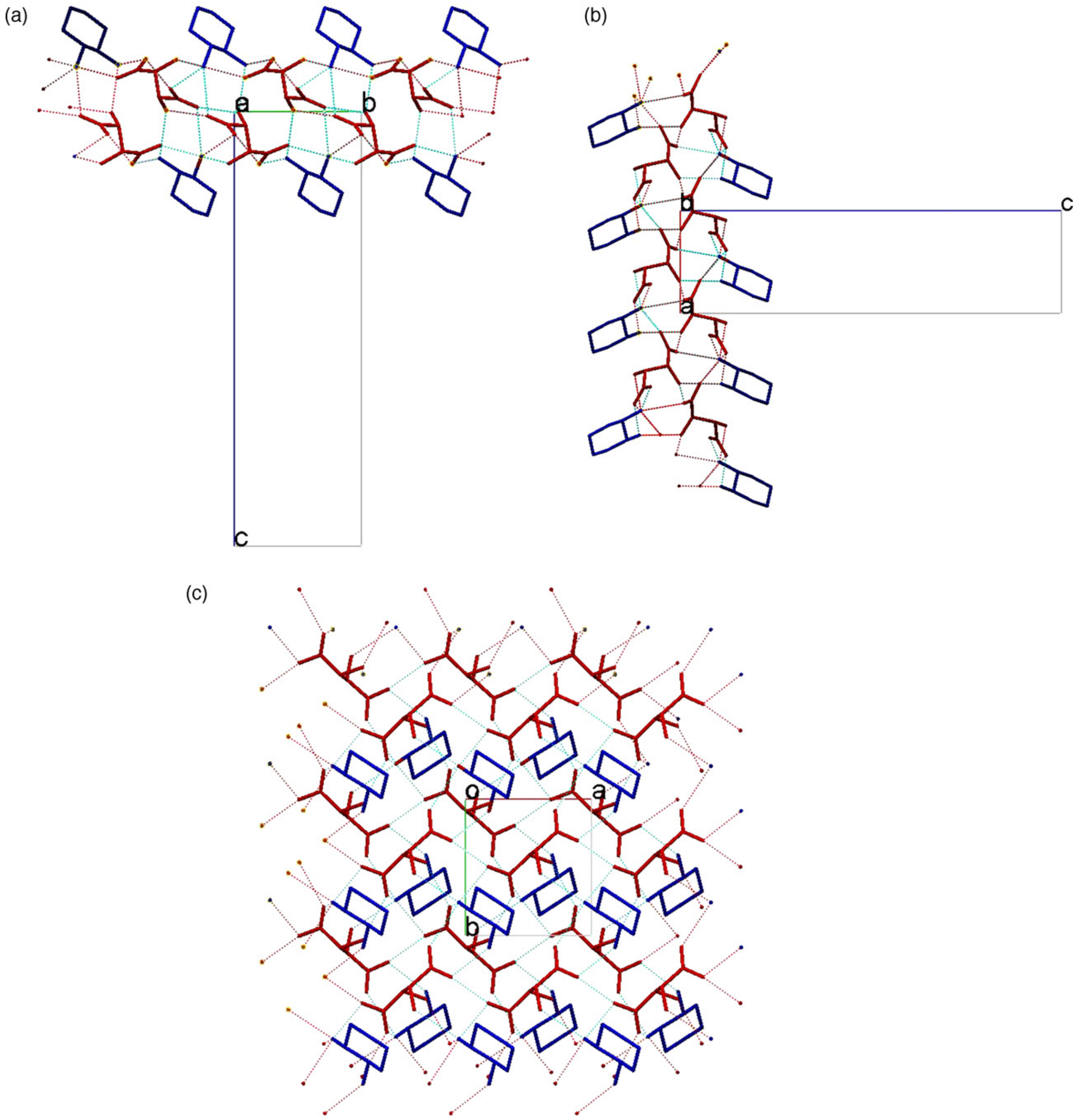

Fig. 3. The two-dimensional infinite hydrogen bonded sheet of the CHD-TA co-crystal (**1**) [26]. Views from the *a*, *b* crystallographic axis, respectively, are side views, while view from the *c* crystallographic axis is a perpendicular view to the sheet. TA is colored red, while CHD is blue. Hydrogen atoms are omitted for clarity.

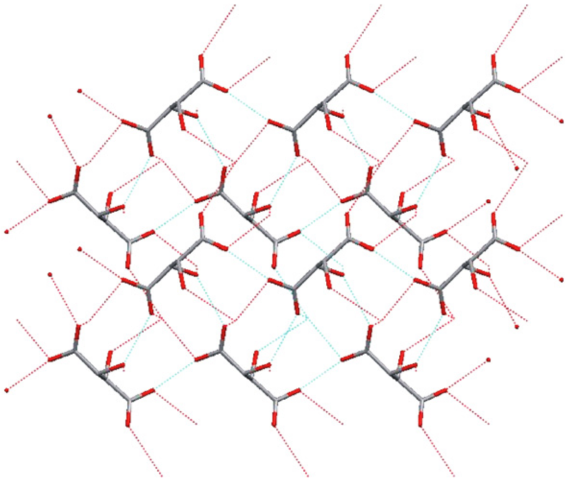

Fig. 4. The inner TA layer of the sheet presenting [26] its hydrogen bonding system of co-crystal 1. View from the *c* crystallographic axis. Hydrogen atoms are omitted for clarity.

an equimolar solution of TA and (*R*,*R*)-CHD in 1:1 (v/v) water and ethanol solvent mixture at room temperature.

The samples of the binary mixtures of TA and enantiomeric CHDs were prepared by evaporation of the solvent from the ethanolic solutions of CHD and TA at reduced pressure (about 160 Torr) and 40–45 °C.

2.2. Single crystal X-ray diffraction

The selected transparent crystal of **1** for single crystal X-ray diffraction measurement had the size of 0.55 mm × 0.55 mm × 0.34 mm. **1** was mounted on a loop with parathon oil. Cell parameters were determined by least-squares of all reflections in the whole measured θ range. Intensity data were collected on a Rigaku Raxis-Rapid diffractometer (graphite monochromator; Mo-Kα radiation, $\lambda = 0.71073$ Å). Empirical absorption correction was applied to the data. The structure was solved by direct methods [20]. Anisotropic full-matrix least-squares refinements [21,22] on F^2 for all non-hydrogen atoms were performed. Neutral atomic scattering factors were taken from the International Tables for X-ray Crystallography [23]. Crystallographic data, parameters of data collection, structure solution and refinement can be found in Table 1. Since there are no strong anomalous scattering centres in the constituents and the diffraction measurement was performed using Mo-Kα radiation, the Flack *x* parameter [24] is not reliable. The O–H hydrogen atomic positions could be located in the difference Fourier maps. Hydrogen atoms were included in structure factor calculations but they were not refined. The isotropic displacement parameters of the hydrogen atoms were approximated from the *U*(eq) value of the atom, to which they were bonded.

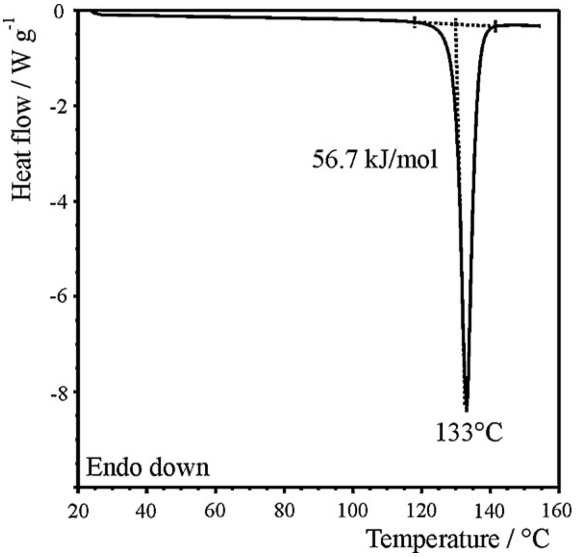

Fig. 6. DSC melting peak of the pure CHD-TA co-crystal (**1**) in sealed Al-pan at 10 °C/min (mass 2.59 mg).

Crystallographic data (excluding structure factors) for the co-crystal structure of **1** have been deposited with the Cambridge Crystallographic Data Centre as supplementary publication number CCDC 728882.

2.3. Further analytical methods

FTIR spectra of co-crystal (**1**) was measured by Excalibur Series FTS 3000 (Biorad) FTIR spectrophotometer in KBr between 700 and 4000 cm^{-1}.

Powder X-ray diffraction patterns were recorded with a PANalytical X'pert Pro MDP X-ray diffractometer using Cu-Kα radiation and Ni filter.

Differential scanning calorimetry (DSC) measurements were performed using a Modulated DSC 2920 device (TA Instruments). The samples (1–2 mg) were measured in sealed Al-pans at a heat-

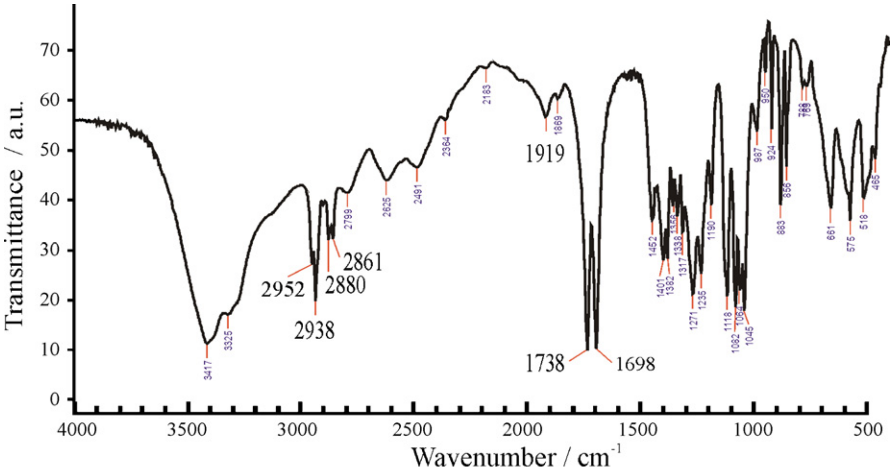

Fig. 5. FTIR spectrum of the CHD-TA co-crystal (**1**).

ing rate of 10 K/min. For temperature and enthalpy calibration of the DSC instrument pure In metal standard was applied. Simultaneous thermogravimetry and differential thermal analysis (TG/DTA) tests were conducted using an STD 2960 Simultaneous TG/DTA equipment (TA Instruments), a heating rate of 10 K/min, open Pt crucibles and an air purge of 130 ml/min. The build-in temperature calibration of TG/DTA was accepted and applied.

3. Results

3.1. The crystal structure of the co-crystal of (+)-tartaric acid and (R,R)-CHD 1:1 (**1**)

The co-crystal **1** crystallizes in the orthorhombic crystal system, space group $P2_12_12_1$ (No 19), having one TA and one CHD molecules in the asymmetric unit ($Z = 4$, $Z' = 1$) (Fig. 2). Detailed crystallographic data, the parameters of data collection, structure determination and refinement are presented in Table 1. As the configuration of the starting material (2*R*,3*R*)-tartaric acid was known (C2 and C3 are R), consequently the configuration of CHD is (*R*,*R*)-1,2-cyclohexanediol (C21 and C26 are R) in the crystal structure. Both alcoholic oxygen atoms in the CHD are in equatorial positions.

The two molecules forming the co-crystal present 4 alcohol and 2 carboxylic acid moieties so the co-crystal contains six donors and eight acceptors for the hydrogen bonds. Thus, a rather complex hydrogen-bonding pattern (Table 2) is constructed in the crystal structure (Fig. 3) A two-dimensional sheet is formed in the ab crystallographic plane with the width of *c*/2. The 2D hydrogen bonded sheet is like a “double sandwich”. The inner part is constructed from a double layer of TA-s (Fig. 4). It is “covered” on both upper and lower sides by the polar moities, the hydroxyl groups of CHD (Fig. 3a and b) while the cyclohexane moieties points outward. Thus the inner part is hydrophilic, the outer coat is hydrophobic.

There are two intramolecular hydrogen bonded loops in TA stabilizing the conformation of the molecule: ···O12–C1–C2–O2–H2O··· and ···O41–C4–C3–O3–H3O···, both are S(5) by the graph set analysis [27]. Within the asymmetric unit the two constituents are hydrogen bonded forming a $R^2{}_2(9)$ homodromic loop: ···O11=C1–O12–H12O···O21–C21–C26–O26–H26···. A further hydrogen bonded loop exists between CHD and TA: ···H21O–O21–C21–C26–O26–H26O···O41=C4–C3–O3···, which is heterodromic $R^2{}_2(10)$. In the inner part of the “sandwich” the TA molecules are connected by strong intermolecular interaction to each other (Fig. 4) and to CHD molecules. There is no hydrogen bond between CHD molecules. One TA molecule within the sheet is connected to four other TA-s, to three TA-s directly, to one TA via a CHD. One TA molecule is connected to four CHD molecules with six hydrogen bonds. The hydrogen bond loops are: ···H3O–O3–C3–C2–O2–H2O···O26–H26···O41··· $R^2{}_3(9)$ and ···O41–C4–C3–O3–H3O···O41=C4–O42–H42···O26–H26··· $R^3{}_3(11)$. Finally, there is a weak C-H···O type interaction also, i.e. C2–H2···O21 within the sheet.

3.2. Characterization of the 1:1 co-crystal of (+)-tartaric acid and (R,R)-CHD (1) by FTIR, DSC and simultaneous TG/DTA

The FTIR spectrum of the co-crystal (**1**) presents an interesting feature (Fig. 5), i.e. a splitting of the single carbonyl C=O stretching vibration (at 1740 cm^{-1}) of pure TA. Indeed, there are two C=O bands at 1738 and 1698 cm^{-1} in the spectrum of co-crystal **1**. The former band (1738 cm^{-1}) belongs certainly to the C4O41O42H42 carboxylic group, despite its carbonyl oxygen O41 is involved in three relatively strong hydrogen bonds as acceptor. Nevertheless its H42 proton is kept also relatively strongly, based on donor–acceptor distances (Table 2). The latter band (at 1698 cm^{-1}) should belong to C1O11O12H12 carboxylic group, whose O11 oxygen is involved only in one weak hydrogen bond, meanwhile the H12 proton is also loosely kept and very intensely shared with O21 oxygen of O21H21 hydroxyl group of CHD. This quasi-anionic feature (which is stabilized by the strong intramolecular hydrogen bond of O12–O2 of O2H2 hydroxyl group absorbing at 1919 cm^{-1}) results in large decrease of carbonyl frequency. Our assignments of the relative strength of hydrogen bonds are based simply on the donor acceptor distances.

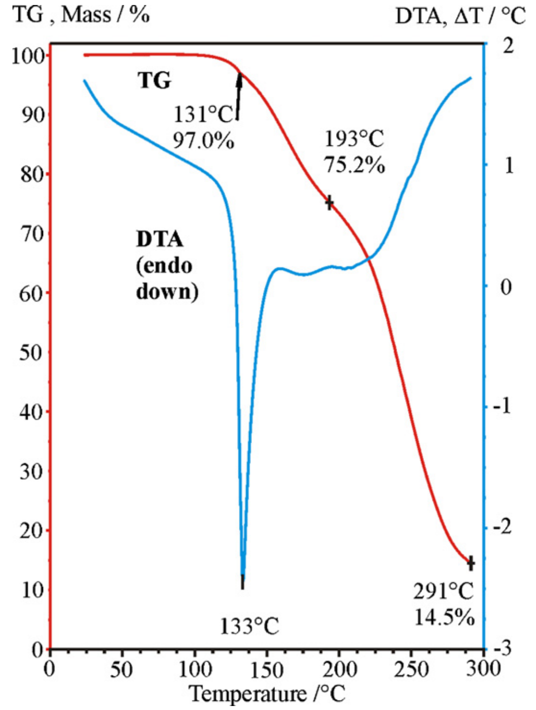

Fig. 7. Simultaneous TG/DTA curves of the pure CHD-TA co-crystal 1 (open Pt crucible, air flow of 130 ml/min, heating rate 10 °C/min, mass 8.68 mg).

The DSC analysis of CHD-TA co-crystal (**1**) in sealed Al-pan showed a melting point at 133.2 °C and its enthalpy of fusion was 56.7 kJ/mol (Fig. 6).

According to simultaneous TG/DTA measurement in an open Pt crucible (Fig. 7), the co-crystal **1** shows nearly same melting point (133 °C). Mass loss of 3% in the TG curve shows partial sublimation of CHD starting from 100 °C till the melting point. A further evaporation of CHD seems to be overlapping with the decomposition process of tartaric acid above 171 °C.

3.3. Differential scanning calorimetry (DSC) and powder X-ray diffraction (XRD) study of the various binary mixtures in the ternary system of solids

Attempt has been made to study in details the phase relations of the three basic components ((*R*,*R*)-CHD, (*S*,*S*)-CHD, and (*R*,*R*)-TA), in order to support the resolution of (±)-*trans*-1,2-cyclohexanediol. The available thermal and structural information on the racemic and enatiomeric *trans*-1,2-cyclohexanediol isomers are summarized in a recent study of Lloyd et al. [28]. The corresponding structural reference data obtained from previous X-ray diffraction studies [18,28–34] are listed in the Supplementary material.

Earlier, CHD was the subject of several publications because of its industrial importance and also different features very interesting to a theoretic point of view. The pure enantiomers crystallized in two different forms that melted at 382.5 K and 352.8 K, and the

Table 3
Melting point and enthalpy of fusion of the chemicals applied in the study of binary systems.

Initial chemicals[a]	T_{fus} observed by DSC K (°C)	ΔH_{fus} measured by DSC (kJ/mol)	Reference T_{fus} (K)	Refs.
(±)-CHD	372 (99) (small pre-melting endothermic peak at 87 °C, as well)	34.4	376.4	[36]
(*R*,*R*)-CHD	381 (108)	18.0	382.5	[36]
(*S*,*S*)-CHD	377 (104)	15.0	Ibid.	Ibid.
(*R*,*R*)-tartaric acid	444 (171) (decomposes)	22.4 (estimated)		[38–40]
Co-crystal (**1**)	406 (133)	56.7		This work

[a] Chemicals listed in the experimental part were used without further purification, and their experimentally measured parameters were involved in the calculations.

Table 4
DSC and XRD data of binary mixtures in the ternary system.

	Binary mixtures	Molar ratio	Eutectic temperature T_{eu} (K/°C)	Liquidus temperature T_{eu} (K/°C)	Crystalline phases present (XRD)
1	(*R*,*R*)-CHD:(*R*,*R*)-TA	2:1	373.3/100.2	Ca. 396/123	(*R*,*R*)-CHD and co-crystal (**1**)
2	(*R*,*R*)-CHD:(*R*,*R*)-TA	1:2	404.7/131.6	Ca. 433/160	Co-crystal (**1**) and (*R*,*R*)-TA
3	(*S*,*S*)-CHD:(*R*,*R*)-TA	3:1	359.7/86.6	–	(*S*,*S*)-CHD and (*R*,*R*)-TA
4	(*S*,*S*)-CHD:(*R*,*R*)-TA	1:1	358.6/85.5	Ca. 410/137	(*S*,*S*)-CHD and (*R*,*R*)-TA
5	(*S*,*S*)-CHD:(*R*,*R*)-TA	1:3	257.2/84.1	Ca. 427/154	(*R*,*R*)-TA and (*S*,*S*)-CHD

crystal were generally a mixture of the two forms whose difference in melting could be observed [35]. Only the stable polymorph's structure was determined [18,28]. The racemic compound ((±)-CHD) of (*R*,*R*)- and (*S*,*S*)-1,2-cyclohexanediol is present under two polymorphic forms, as well. The stable polymorph's structure was determined in [28,31,32] and the metastable's in [28].

The solid–liquid melting phase diagram for mixtures of (*R*,*R*)-CHD and (*S*,*S*)-CHD was investigated by DSC method [36]. This binary system resembled a type of melting phase diagram including a racemic compound [37], but had an unusual feature. Usually, a racemic compound, as a co-crystal of both enantiomers, can form a eutectic mixture, i.e. crystal conglomerate with one of the enantiomers. Actually, in this case, eutectic compositions were found at about molar fractions of $x_{SS\text{-}CHD} = 0.2$ and 0.8. Furthermore the corresponding eutectic temperature of $T_{eu} = 371$ K was observed in the composition ranges $0 < x_{SS\text{-}CHD} < 0.2$ and $0.8 < x_{SS\text{-}CHD} < 1$, but in intermediate composition, $0.2 < x_{SS\text{-}CHD} < 0.8$, no eutectic melting endothermic heat effect occurred at all [33]. This phenomenon was explained by Leitao et al. as solid solution formation for compositions within the latter wide range around the 1:1 molar ratio. A metastable phase was also found below eutectic temperature ($x_{SS\text{-}CHD} < 0.2$ and $x_{SS\text{-}CHD} > 0.8$), as the continuation of the liquidus curve of solid solution [36].

Now, we have investigated both binary systems between (*R*,*R*)-TA and (*R*,*R*)-CHD or (*S*,*S*)-CHD with DSC and powder X-ray diffraction, with help of samples prepared at representative 1:3, 1:1, and 3:1 molar ratios. The melting point and enthalpy of fusion of the initial chemicals applied in preparation and calculation of binary mixtures are listed in Table 3, while the temperatures of the observed thermal heat effect(s) and the initial crystalline phase composition of various mixtures at room temperature are summarized in Table 4.

The experimental powder X-ray diffraction pattern of sample with 1:1 molar ratio of (*R*,*R*)-CHD and (*R*,*R*)-TA has been checked with comparison with the simulated powder diffraction pattern of co-crystal CHD-TA (**1**) generated from the single crystal data presented above: the agreement was perfect.

The XRD profile of the samples formed from the 1:2 and 2:1 binary mixtures of (*R*,*R*)-CHD and (*R*,*R*)-TA corresponded to the 1:1 mixtures of co-crystal (**1**) and (*R*,*R*)-CHD or (*R*,*R*)-TA, respectively. These samples showed eutectic melting behavior, eutectic temperatures were found lower than the melting point of co-crystal (**1**) by DSC. The first eutectic is found between (*R*,*R*)-CHD and co-crystal (**1**) at 100 °C (Fig. 8a); and the second between co-crystal (**1**) and (*R*,*R*)-TA at 131.6 °C. DSC showed, in all the cases of the binary (*S*,*S*)-CHD–(*R*,*R*)-TA system, a constant eutectic temperature of 84–86 °C. It is lower than the melting point of (*S*,*S*)-CHD and the eutectic temperature of (**1**) and TA or (**1**) and (*R*,*R*)-CHD. This indicates that no co-crystal is formed between (*S*,*S*)-CHD and (*R*,*R*)-TA. This result is corroborating with the XRD profile of the samples for the binary mixtures of (*R*,*R*)-TA and (*S*,*S*)-CHD of 1:3, 1:1, and 3:1 molar ratio, presenting only patterns of (*R*,*R*)-tartaric acid (PDF No. 00-033-1883; 00-020-1901; 00-031-1911) and (*S*,*S*)-CHD (PDF No. 02-093-3042), and no other reflections occurred.

After the eutectic melting the elongated dissolution of the excess phase continued, as it is shown for both mixture of the 1:1 molar ratio of (*R*,*R*)-CHD and co-crystal (**1**) or (*S*,*S*)-CHD and (*R*,*R*)-TA in Fig. 8a and b, respectively. In case of 3:1 molar ratio of (*S*,*S*)-CHD and (*R*,*R*)-TA, only the single eutectic melting effect occurred, i.e. it represents almost a eutectic composition between (*S*,*S*)-CHD and (*R*,*R*)-TA.

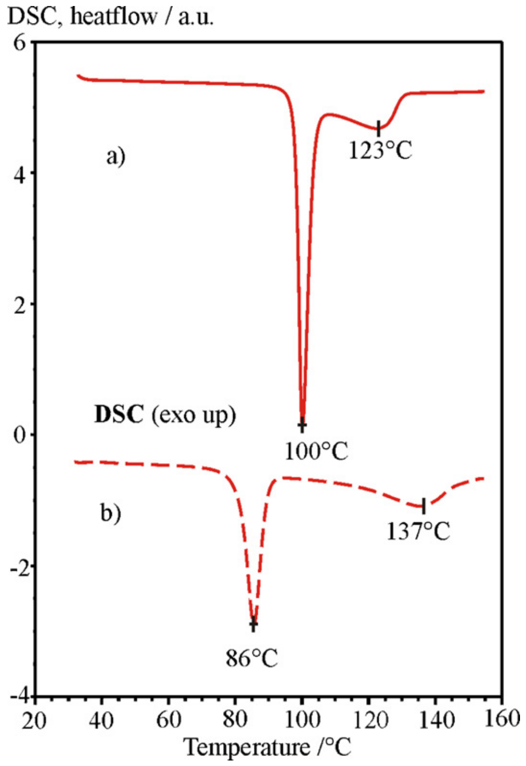

Fig. 8. DSC curve of binary mixtures corresponding to 1:1 molar ratio of -a) (*R*,*R*)-CHD and co-crystal (**1**) and b) (*S*,*S*)-CHD and (*R*,*R*)-TA, both exhibiting eutectic melting behavior.

Table 5
Calculated eutectic compositions, calculated and measured eutectic temperatures of binary and ternary mixtures (based on experimental DSC data of used chemicals and assumption of validity of Schöder–van Laar equation).

Components	Calculated eutectic molar fractions	Calculated eutectic temperature (K, °C)	Measured eutectic temperature (K, °C)
Co-crystal (**1**)/(*R*,*R*)-CHD	$x_{(\mathbf{1})}=0.184$ $x_{RR\text{-}CHD}=0.816$	369, 96	373, 100
Co-crystal (**1**)/(*R*,*R*)-TA	$x_{(\mathbf{1})}=0.553$ $x_{RR\text{-}TA}=0.447$	392, 119	404, 131
(*R*,*R*)-TA/(*S*,*S*)-CHD	$x_{RR\text{-}TA}=0.148$ $x_{SS\text{-}CHD}=0.852$	365, 92	359, 86
(*R*,*R*)-CHD (or (*S*,*S*)-CHD)/racemic-CHD	$x_{RR\text{-}CHD}=0.222$ $x_{(\pm)\text{-}CHD}=0778$	366, 93 (Prigogine-Defay equation also applied)	371, 98
Co-crystal (**1**)/racemic-CHD	$x_{(\mathbf{1})}=0.134$ $x_{(\pm)\text{-}CHD}=0.866$	363, 90	Not measured
Co-crystal (**1**)/(*R*,*R*)-TA/(*S*,*S*)-CHD	$x_{(\mathbf{1})}=0.077$ $x_{RR\text{-}TA}=0.206$ $x_{SS\text{-}CHD}=0.717$	353, 80	Not measured
Co-crystal (**1**)/(*R*,*R*)-CHD (or (*S*,*S*)-CHD)/racemic-CHD	$x_{(\mathbf{1})}=0.051$ $x_{RR\text{-}CHD}=0.542$ $x_{(\pm)\text{-}CHD}=0.405$	345, 72	Not measured

Estimation of eutectic molar fraction, eutectic temperature, and liquidus curves of binary eutectic phase diagrams have also been calculated numerically [41,42] based on the temperature and enthalpy of fusion of pure crystalline phases (listed in Table 3) assuming the validity of simplified Schröder–van Laar equation, and in case of racemate also of Prigogine–Defay–Mauser equation [37]. Beyond the results on various binary subsystems, the calculated eutectic parameters for ternary eutectic subsystems, with assumption of incompatibility of (*R*,*R*)-TA and racemic CHD, and according to the Schröder–van Laar equation [43] are also reported in Table 5. A schematic diagram of phase relation of the three-component ((*R*,*R*)-CHD, (*S*,*S*)-CHD, and (*R*,*R*)-TA) system, that allows the required resolution, is exhibited in Fig. 9.

Based on the result presented above, resolution experiments were performed with (*R*,*R*)-TA: (*S*,*S*)-CHD: (*R*,*R*)-CHD = 2:0.5: 0.5 molar ratio. Results showed significant improvement of the process, in one single resolution step (including sample preparation, supercritical carbon dioxide extraction at optimal conditions and complexed CHD liberation): enantiomeric excess of 85% (yield 45%) and 88.9% (yield 50.2%) for (*S*,*S*)-CHD and (*R*,*R*)-CHD, respectively.

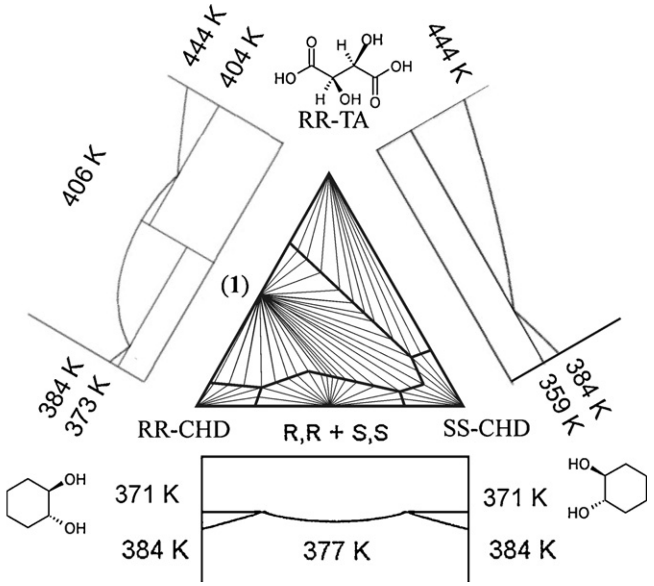

Fig. 9. Schematic three-component *T*–*x* phase diagram for *trans*-1,2-cyclohexanediols and (*R*,*R*)-tartaric acid, drawn from the data shown in Table 5. Schematic *T*–*x* diagrams for each pair of components are also shown. (**1**) corresponds to the co-crystal of (*R*,*R*)-1,2-cyclohexanediol and (*R*,*R*)-tartaric acid (1:1). No phase containing (*S*,*S*)-1,2-cyclohexanediol and (*R*,*R*)-tartaric acid is known.

4. Conclusion

The structure of **1**, 1:1 co-crystal of (*R*,*R*)-TA and (*R*,*R*)-CHD (orthorhombic crystal system, space group $P2_12_12_1$) has been determined by single crystal X-ray diffraction. The crystal structure is made of layers, each formed of four sheets, CHD-TA-TA-CHD. The inner part of the layer is polar (alcoholic and carboxylic groups of TA and alcohol groups of CHD) whereas the outside is apolar (cyclohexane rings of CHD). The co-crystal melts at 133 °C and its sublimation starts at 100 °C. In the case of the binary mixtures between (*R*,*R*)-CHD and TA, two different eutectic temperatures were found, the first one between (*R*,*R*)-CHD and co-crystal (at 100 °C) and the second between co-crystal and TA (at 131 °C), whereas, in the case of the binary (*S*,*S*)-CHD-TA, the constant eutectic temperature (84–86 °C) helps to conclude that no co-crystal was formed, which result was corroborated by powder X-ray diffraction. Further improvement of resolution technique by supercritical carbondioxide based on the explored phase relations is under completion.

Acknowledgements

This research work was financially supported through a European Community Marie Curie Fellowship (Project MEST-CT-2004-007767, for further information: http://www.cordis.lu/improving) and by the Hungarian Scientific Research Fund (OTKA 72861). P.B. and L.P. acknowledge the National Science and Technology Office for an X-Ray diffractometer purchase grant (MU-00338/2003). J.M., Sz.I.M., and G.P. also thank for the purchase grant of a new HT-XRD apparatus supported by the EU and the Hungarian government (GVOP-3.2.1.-2004-0224, KMA). The authors thank Prof Mátyás Czugler for giving the opportunity to carry out the single crystal XRD measurement that allowed the determination of the structure.

Appendix A. Supplementary data

Supplementary data associated with this article can be found, in the online version, at doi:10.1016/j.tca.2009.09.001.

References

[1] A.N. Collins, C.N. Sheldrake, J. Crosby, Chirality in Industry—An Overview, John Wiley & Sons, Chischester, 1992.

[2] L. Synoradzki, U. Bernas, P. Ruskowski, Org. Prep. Proced. Int. 40 (2008) 163–200.
[3] K. Nemák, M. Acs, Z.M. Jászay, D. Kozma, E. Fogassy, Tetrahedron 52 (1996) 1637–1642.
[4] R. Illés, C. Kassai, G. Pokol, E. Fogassy, D. Kozma, J. Therm. Anal. Calorim. 68 (2002) 679–685.
[5] C. Kassai, Z. Juvancz, J. Bálint, E. Fogassy, D. Kozma, Tetrahedron 56 (2000) 8355–8359.
[6] C. Kassai, R. Illés, G. Pokol, J. Sztatisz, E. Fogassy, D. Kozma, J. Therm. Anal. Calorim. 62 (2000) 647–655.
[7] H. Simon, K. Marthi, G. Pokol, E. Fogassy, D. Kozma, J. Therm. Anal. Calorim. 74 (2003) 155–162.
[8] R. Illés, C. Kassai, G. Pokol, J. Madarász, E. Fogassy, D. Kozma, J. Therm. Anal. Calorim. 61 (2000) 745–755.
[9] M.D. Groaning, B.J. Rowe, C.D. Spilling, Tetrahedron Lett. 39 (1998) 5485–5488.
[10] M. Tanaka, M. Oba, K. Tamai, H. Suemune, J. Org. Chem. 66 (2001) 2667–2673.
[11] E. Wojaczynska, J. Skarzewski, Tetrahedron Asymmetry 19 (2008) 593–597.
[12] P. Molnár, P. Thorey, G. Bánsághi, E. Székely, L. Poppe, A. Tomin, S. Kemény, E. Fogassy, B. Simándi, Tetrahedron Asymmetry 19 (2008) 1587–1592.
[13] P.G. Jessop, W. Leitner, Chemical Synthesis Using Supercritical Fluids, Wiley–VCH Verlag GmbH, Weinheim, 1999.
[14] M. McHugh, V. Krukonis, Supercritical Fluid Extraction: Principles and Practice, 2nd ed, Butterworth–Heinemann, Boston, 1994.
[15] M. Kawashima, A. Hirayama, Chem. Lett. (1991) 763–766.
[16] S. Hanessian, M. Simard, S. Roelens, J. Am. Chem. Soc. 117 (1995) 7630–7645.
[17] S. Hanessian, R. Saladino, R. Margarita, M. Simard, Chem. Eur. J. 5 (1999) 2169–2183.
[18] S. Hanessian, A. Gomtsyan, M. Simard, S. Roelens, J. Am. Chem. Soc. 116 (1994) 4495–4496.
[19] H. Chanzy, E. Maia, S. Perez, Acta Cryst. B38 (1982) 852–855.
[20] G.M. Sheldrick, SHELXS-97 Program for Crystal Structures Solution, University of Göttingen, Göttingen, 1997.
[21] L.J. Barbour, J. Supramol. Chem. 1 (2001) 189–191.
[22] G.M. Sheldrick, SHELXL-97 Program for the Refinement of Crystal Structures, University of Göttingen, Göttingen, 1997.
[23] A.J.C. Wilson, International Tables for X-ray Crystallography, Kluwer Academic Publishers, Dordrecht, 1992.
[24] H.D. Flack, Acta Crystallogr. A: Found. Crystallogr. 39 (1983) 876–881.
[25] A.L. Spek, J. Appl. Crystallogr. 36 (2003) 7–13.
[26] C.F. Macrae, P.R. Edgington, P. McCabe, E. Pidcock, G.P. Shields, R. Taylor, M. Towler, J.V.D. Streek, J. Appl. Crystallogr. 39 (2006) 453–457.
[27] J. Grell, J. Bernstein, G. Tinhofer, Acta Crystallogr. B: Struct. Sci. 56 (2000) 166–1166.
[28] M.A. Lloyd, G.E. Patterson, G.H. Simpson, L.L. Duncan, D.P. King, Y. Fu, B.O. Patrick, S. Parkin, C.P. Brock, Acta Crystallogr. B: Struct. Sci. B63 (2007) 433–447.
[29] F.H. Allen, Acta Crystallogr. B: Struct. Sci. 58 (2002) 380–388.
[30] International Centre for Diffraction Data (ICDD), Powder Diffraction File PDF-2 Release 2008.
[31] R. Sillanpaa, M. Leskela, L. Hiltunen, Acta Chem. Scand. A B38 (1984) 249–254.
[32] P.G. Jones, M.R. Edwards, A.J. Kirby, Acta Crystallogr. C: Cryst. Struct. Commun. C45 (1989) 244–246.
[33] R.T. Stibrany, J.A. Potenza, Private communication to CCDC (2007), as contribution from Dept. of Chemical Biology, Rutgers, The State University of New Yersey.
[34] D. Schultz, G. McCarthy, North Dakota State University, USA, ICDD Grant-in-Aid, 1986.
[35] M.L.P. Leitao, R.A.E. Castro, F.S. Costa, J.S. Redinha, Thermochim. Acta 378 (2001) 117–124.
[36] M.L.P. Leitao, M.E. Eusebio, T.M.R. Maria, J.S. Redinha, J. Chem. Thermodyn. 34 (2002) 557–568.
[37] J. Jacques, A. Collet, S.H. Wilen, Enantiomers, Racemates, and Resolution, John Wiley & Sons, New York, 1981.
[38] S.A. Martin Britto Dhas, M. Suresh, G. Bhagavannarayana, S. Natarajan, J. Cryst. Growth 309 (2007) 48–52.
[39] N. Takata, K. Shiraki, R. Takano, Y. Hayashi, K. Terada, Cryst. Growth Des. 8 (2008) 3032–3037.
[40] M.K. Stanton, A. Bak, Cryst. Growth Des. 8 (2008) 3856–3862.
[41] D. Kozma, G. Pokol, M. Ács, J. Chem. Soc., Perkin Trans. 2 (1992) 435.
[42] J. Madarász, D. Kozma, G. Pokol, M. Ács, E. Fogassy, J. Therm. Anal. Calorim. 42 (1994) 877–894.
[43] A.A. Smith, Tetrahedron Asymmetry 9 (1998) 2925–2937.